

Thermal activation of carriers from a metallic impurity band

S. Liu, K. Karrai, F. Dunmore, and H. D. Drew

Department of Physics, University of Maryland, College Park, Maryland 20742

R. Wilson

Laboratory for Physical Sciences, College Park, Maryland 20740

G. A. Thomas

AT&T Bell Lab, Murray Hill, New Jersey 07974

(Received 11 February 1993; revised manuscript received 15 June 1993)

Transport and far-infrared transmission measurements are reported on Si-doped GaAs epitaxial films ($n \gtrsim$ the Mott density n_0). The spectra display a $1s \rightarrow 2p$ resonance and a Drude response that persists to low temperatures. An analysis of the temperature dependence of the spectra gives the activation energy for thermal excitation of carriers from the metallic impurity band to the conduction band. The effective mass of the impurity band m_i is obtained from optical sum-rule considerations. m_i appears to diverge at the metal-insulator transition. The large m_i implies a correlation-induced narrowing of the impurity band. The activation energy E_a and effective mass m_i obtained from optical measurements are consistent with the results obtained from transport measurements. The transmission spectra of Si:P and planar Si-doped GaAs/Al_xGa_{1-x}As superlattices are also discussed.

Semiconductors doped with shallow impurities undergo a metal-to-insulator transition at $T=0$ when the impurity density decreases below a critical value n_0 . Because this phase transition involves both electron correlations and disorder, this phenomenon presents interesting theoretical problems and the subject has been extensively studied.^{1,2} Despite considerable progress the nature of the electronic structure of these heavily doped semiconductors is only partially understood. This problem has taken on new importance with the advent of high-temperature superconductivity in the layered cuprates. It is known that the superconductivity in these materials occurs under conditions that are close to the metal-insulator transition (MIT).³ For the case of Si-doped GaAs recent experiments have produced convincing evidence indicating that near the MIT the conduction takes place in a metallic impurity band.^{4,5} Far-infrared magnetotransmission measurements on GaAs doped with Si ($n \lesssim 5n_0$) have demonstrated a resonance associated with the $1s-2p$ transition in the donors even when the samples are metallic as determined by transport measurements. In this paper we present a detailed study of the temperature dependence of the optical response of Si-doped GaAs in zero magnetic field. These data together with magnetotransport measurements can be consistently interpreted in terms of thermal excitation of carriers from the metallic impurity band to the conduction band. We determine the activation energies and impurity band effective mass as a function of donor density. We also present data on GaAs doped with planar Si layers and bulk Si doped with P. Planar-doped GaAs behaves similarly to uniformly doped bulk GaAs but the metallic impurity band appears more robust in two dimensions than in three dimensions. In the case of P-doped Si, there is no evidence for $1s-2p$ transitions for $n \geq n_0$.

The samples used in this study were 2–3- μm -thick Si-doped GaAs films grown on semi-insulating GaAs substrates by molecular-beam epitaxy. Transport measurements were made on specimens that were photolithographically patterned into $0.5 \times 3\text{-mm}$ Hall bars, and contacted with annealed indium. Carrier densities, compensations, and mobilities were deduced from low-field Hall measurements performed at room temperature, 77 and 4.2 K.⁵ The densities on several samples were also checked by CV measurements, and the results agreed well with those of the transport measurements.⁵ Measurements of ρ_{xx} , ρ_{xy} , and ρ_{zz} were made by the ac technique for temperatures down to 0.36 K and magnetic fields up to 9.2 T. The critical fields B_c of the magnetic-field-induced metal-insulator transition were determined by extrapolating the conductivity $\sigma_{zz}(B)$ to zero temperature. Although the weak-field Hall effect was temperature dependent, for the metallic samples the Hall coefficient at 4.2 and 300 K were found to be equal to within the experimental error of $\cong 3\%$. We have also observed and studied the Shubnikov-de Haas effect in ρ_{xx} and ρ_{zz} for all of the metallic samples.⁵

The far-infrared transmission spectra were measured as a function of temperature at zero magnetic field using a Bomem DA3 Fourier-transform infrared spectrometer with a Si composite bolometer operating at 2 K. The sample and a reference semi-insulating GaAs substrate were mounted on apertures in a two-position sample holder. The sample temperature was measured by a Si diode thermometer glued on the aperture near the sample. The sample and reference could be switched into the IR beam with an externally controlled manipulator. Both the sample and the reference substrates were wedged 4° to avoid interference effects in a measured spectra. The measured quantity is the ratio of the

transmission of the sample to that of the reference.

Figure 1 shows the transmission spectra of sample *A* at 12 and 82 K measured at zero magnetic field, where the sample is metallic. The carrier density of this sample is $1.6 \times 10^{16} \text{ cm}^{-3}$, which is just above the MIT critical density n_0 ($1.5 \times 10^{16} \text{ cm}^{-3}$). The critical field B_c of the metal-insulator transition, deduced from the low-temperature transport measurements for this sample, is 3.1 T. At 12 K the transmission spectrum is seen to be dominated by the $1s$ - $2p$ donor transition. At 82 K, however, the transmission spectrum displays a free-electron Drude behavior. Transmission spectra were also measured at intermediate temperatures. As the temperature is raised above 12 K the spectra transform continuously from the $1s$ - $2p$ line shape to the Drude curve.

We have analyzed these data using a Lorentz oscillator model conductivity function to fit the transmission spectra

$$\sigma(\omega, T) = \frac{ne^2}{m_b} \left[\frac{f_{sp}(T)i\omega}{\omega_0^2 - \omega^2 + i\omega\tau_{sp}^{-1}} + \frac{f_D(T)}{i\omega + \tau_D^{-1}} \right].$$

The first term is a bound-state oscillator used to model the $1s$ - $2p$ absorption, and the second term is a Drude term. The τ^{-1} 's are their linewidths, the f 's are the oscillator strengths, n is the carrier density, taken as the room-temperature Hall density, and $m_b = 0.067m_0$ is the conduction-band effective mass in GaAs. For isolated hydrogenic donors, most of the oscillator strength sum rule is contained in the $1s$ - $2p$ transition. For simplicity, and because the other bound-state transition would be overlapping for the broad lines observed in these spectra, we consider only one bound-state Lorentzian. Consequently, the sum-rule condition becomes $f_{sp} + f_D = 1$.

The transmission spectra are calculated from the conductivity using the thin-film relation

$$T(\omega, T) = \frac{4n_s}{|n_s + 1 + Z_0\sigma(\omega, T)d|^2},$$

where $n_s = 3.53$ is the refractive index of the GaAs substrate, d is the film thickness, and Z_0 is the impedance of free space.

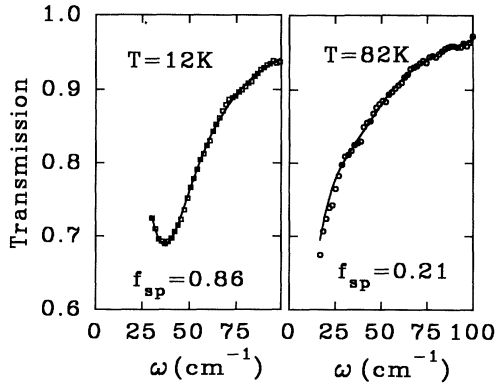


FIG. 1. The transmission spectra of sample *A* at 12 K (left panel) and 82 K (right panel). The open circles are the experimental data and solid curves are the best fits to the oscillator model described in the text.

The free parameters used in the fittings were f_{sp} , the τ 's (found to be equal to within experimental error), and ω_0 . The best fits of the transmission spectra to the oscillator model described above are shown in Fig. 1 as solid curves. For the Drude response dominated spectrum at 82 K, we find $f_{sp} = 0.21$ and $f_D = 0.79$; and for the $1s$ - $2p$ dominated spectrum at 12 K, $f_{sp} = 0.86$, $f_D = 0.14$, and $\omega_0 = 36 \text{ cm}^{-1}$. For isolated Si donors in GaAs the $1s \rightarrow 2p$ absorption is observed at 34.6 cm^{-1} .

It is interesting to note that the oscillator strength of the Drude response f_D remains finite at low temperature since the conduction-band carrier density is expected to be almost zero and nearly all the carriers are in the impurity band. Also, the residual f_D at low temperatures is larger for samples with higher carrier densities. For sample *A*, $f_D = 0.14$ at 12 K and for sample *B* ($n = 2.9 \times 10^{16} \text{ cm}^{-3}$), $f_D = 0.25$ at 4 K. This observation suggests that the impurity band produces the Drude component. Consequently, the Drude response has two components in general, one from the conduction-band carriers and the other from the impurity band. Therefore, we write the Drude oscillator strength as

$$f_D(T) = \frac{n_c(T)}{n} \frac{m_b}{m_c} + \frac{n_i(T)}{n} \frac{m_b}{m_i}.$$

The first term is the conduction-band contribution, the second is that of the impurity band. n_c , n_i and m_c , m_i are the carrier densities and effective masses of the conduction band and the impurity band, respectively. We can simplify this expression by making use of the sum rule on the conductivity and the low-temperature and high-temperature limits of σ . At low temperature, we assume $n_i = n$, $n_c = 0$. This conclusion is consistent with the Hall measurements in which the 4.2- and 300-K Hall coefficients are equal. From this we deduce that $f_D(0) = m_b/m_i$. Therefore, the Drude oscillator strength gives a measure of the impurity band effective mass. At high temperature, where $n_i = 0$, $n_c = n$, the sum rule implies that $m_c = m_b$. Using these results, we can write

$$f_{sp}(T) = \frac{n_i(T)}{n} \left[1 - \frac{m_b}{m_i} \right].$$

In order to analyze the temperature dependence of the oscillator strengths we have modeled the thermal activation of carriers from the impurity band to the conduction band which are assumed to be separated by an energy E_a . We use the single impurity level model and forbid double occupancy. Using this thermal model and the oscillator strength relations discussed above we have fit the temperature dependence of the oscillator strengths with E_a and m_i as fitting parameters.

The temperature dependence of f_{sp} and f_D deduced from the transmission spectra and the results of the model fitting are shown in Fig. 2 for sample *A* and sample *B*. The model is seen to provide an excellent representation of the data. Also shown in the figure, for comparison, is the calculated oscillator strengths using the same activation energies but dropping the impurity band Drude contribution ($m_i = \infty$).

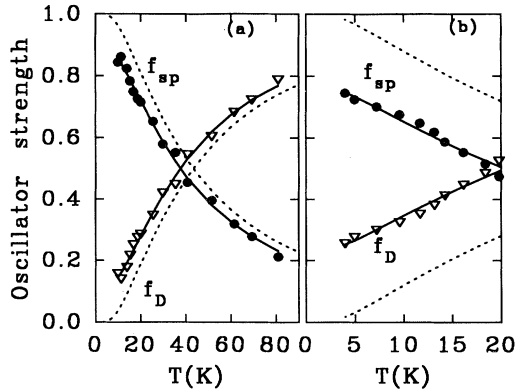


FIG. 2. The temperature dependence of the oscillator strength f_{sp} and f_D deduced from the transmission spectra of sample *A*. The solid circles and open triangles are the data points. The solid curves are the best-fit curves to the thermal activation model described in the text. The parameters of the fits are $m_i=9.5m_b$ and $E_i=4.1$ meV for sample *A* ($n=1.6\times 10^{16}$ cm $^{-3}$) and $m_i=4m_b$ and $E_i=1.8$ meV for sample *B* (2.9×10^{16} cm $^{-3}$). The dashed curves are the calculated results taking $m_i=\infty$ (ignoring the impurity band Drude term).

It is interesting to compare these results with the results from dc transport studies. First we note that $\sigma(\omega=0)$ deduced from the fits agree with the measured value of the 4.2-K dc conductivity to within experimental error ($\pm 30\%$). At low temperatures we have observed a Shubnikov–de Haas (SdH) effect in both ρ_{xx} and ρ_{zz} in these metallic samples. In an earlier publication we reported the analysis of the SdH measurements made at temperatures down to 0.36 K for the effective mass.⁵ The results are reproduced in Fig. 3 together with the results deduced from the optical data. The good agreement further supports the idea of the metallic impurity band in this system. We can also analyze the weak-field magnetotransport in terms of the thermal model presented above.

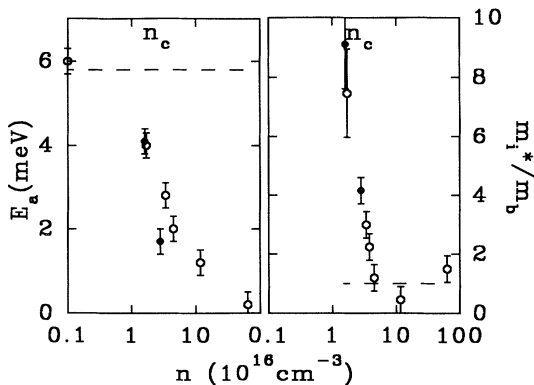


FIG. 3. Right panel: The effective mass of the metallic impurity band relative to the conduction-band mass ($m_b=0.067m_0$) vs carrier density. In both panels the open circles are data obtained from transport measurements and the solid points are obtained from the optical experiments. Left panel: The activation energy as functions of carrier density. The solid line is the isolated donor ionization energy, 5.8 meV.

To analyze the resistivity and Hall coefficient data for n_i , n_c , μ_i , and μ_c we can use the relation $n_i+n_c=n$ but to obtain a unique solution we need another relation. If we assume $\mu_i(T)=\mu_i(0)$, we can perform the analysis and determine E_a for samples with different densities. The results of this analysis are shown in Fig. 3. Alternatively, we could assume that $\tau_i=\tau_c$ as found in the optical data. The resulting values obtained for E_a do not differ appreciably. Neither assumption can be justified; however, they demonstrate that E_a is not very sensitive to μ_i . In the literature the transport data in this range of densities have been discussed in terms of a temperature-dependent Hall factor.⁶ The optical data and the analysis presented here demonstrate that the thermal activation from the impurity band to the conduction band cannot be ignored in this density range. If a Hall factor is used in our analysis the E_a values resulting from the thermal model will decrease, approaching the optical values. We conclude from this analysis that the transport data and the optical data are consistent.

The large m_i observed in samples doped close to the MIT implies a narrow impurity bandwidth W . From the tight-binding theory we can express W as

$$W = \frac{\hbar^2}{2m_b a^2} \frac{m_b}{m_i} 2z, \quad (1)$$

where a is the lattice constant, which we take as the mean interdonor spacing, and z is the number of nearest neighbors for which we take the close-packed lattice value of 6.¹ For $m_i/m_b=10$, corresponding to sample *A*, Eq. (1) gives $W\cong 1$ meV. This implies that the impurity bandwidth is smaller than the activation energy E_a which indicates that the metallic conduction is associated with the lower Hubbard band. On the other hand, this deduced value for W is considerably smaller than that predicted by estimating the tight-binding matrix elements. From this observation we suggest that correlation effects may narrow the impurity band.

The picture that emerges from these results is as follows. For $n < n_0$ the far-IR spectrum is dominated by the $1s \rightarrow 2p$ transition and the intraimpurity band contribution is small (a small photon-induced hopping contribution is also expected). Therefore, $m_b/m_i \rightarrow 0$. Also the dc conductivity has an activation energy close to the isolated Rydberg energy. When n exceeds n_0 the interaction with the donor ions lowers the conduction-band edge and the overlap of the donor wave functions leads to the formation of a band of delocalized states in the (lower Hubbard) impurity band. For $n \cong n_0$ the impurity band is narrow leading to a large impurity band effective mass. As n increases above n_0 the impurity band broadens and merges with the conduction band and the $1s \rightarrow 2p$ transition becomes indistinguishable from the Drude response for $n \gtrsim 5n_0$ so that $m_b/m_i \rightarrow 1$.

We have also investigated impurity band effects in several other semiconductor systems—molecular-beam-epitaxy-grown GaAs doped with a superlattice of Si planes and bulk Si doped with P.⁷ The planar Si superlattice in the GaAs sample has 200 layers with period 64 Å and thickness 11 Å. The Si doping is $n=8\times 10^{10}$

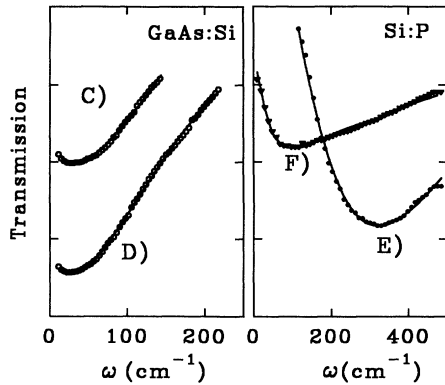


FIG. 4. The transmission spectra at 2.2 K for two other systems. The points are experimental data and solid curves are the best fits using the oscillator model described in the text. *C* and *D* are Si superlattice doped GaAs samples. The Drude oscillator strengths are 0.09 and 0.30, suggesting enhanced effective masses of $10m_0$ and $3.3m_0$, respectively. *E* (insulating) and *F* are bulk P-doped Si samples with densities $n=0.5n_0$ and $n=1.01n_0$. A valley-orbit oscillator term at 100 cm^{-1} was included in the analysis. The Drude strength in both samples was found to be less than the fitting error of $\approx 2\%$.

$\text{cm}^{-2}/\text{layer}$ for sample *C* and $n=2.5 \times 10^{11}\text{ cm}^{-2}/\text{layer}$ for sample *D*. The 2.2-K transmission spectra of several of these samples is shown in Fig. 4. We have analyzed these data using the same model that we employed on the uniformly doped GaAs epitaxial films. The best fits are shown in the figure as solid lines. The Drude oscillator strengths are $f_D=0.09$ for sample *C* and $f_D=0.30$ for sample *D* corresponding to enhanced effective masses $m_i=10m_b$ for sample *C* and $m_i=3.3m_b$ for sample *D*. If these are interpreted as three-dimensional systems, it appears that the impurity band persists to higher density ($n \approx 4 \times 10^{17}\text{ cm}^{-3}$) than was found for the uniformly doped GaAs samples. Measurements on samples with larger periods a ($a \approx 1200\text{ \AA}$) give similar results.^{8,9} Therefore, the impurity band appears to be more robust in two dimensions (2D) than in 3D.

In the case of P-doped Si we have studied one insulating sample *E* ($n=0.5n_c$) and one metallic sample *F* with the donor density slightly higher than the critical density ($n=1.01n_c$).¹⁰ For the insulating sample the spectrum is dominated by the broadened $1s-2p$ transition and there is no evidence of a Drude component. The spectra for the metallic sample cannot be well represented using only a Drude and a $1s-2p$ oscillator in the fitting. There is only a very small $1s-2p$ component (6%) and most of the oscillator strength seems to have been shifted to $\approx 100\text{ cm}^{-1}$. This energy corresponds to the valley-orbit splitting in Si donors. The valley-orbit transition is not dipole active for isolated donors, however it is Raman active. In Raman measurements it has been observed to persist to slightly above n_c .¹¹ The observed shift of the IR oscillator strength suggests that at these high donor densities, wave-function overlap has broken the isolated donor selection rule and enhanced the valley-orbit transition at the expense of the $1s-2p$ transition. Therefore, we used a three-oscillator model to fit the optical data. We take a Drude term, one oscillator at 320 cm^{-1} to model the $1s-2p$ transition and one at 100 cm^{-1} to model the valley-orbit transition. The best-fit curve is shown in Fig. 4. The resulting oscillator strengths are $f_{sp}=0.05$, $f_{vo}=0.93$, $f_D \approx 0.02$ ($m_i \approx 50m_b$). The Drude component is at the limit of our fitting error; ± 0.02 . This result is consistent with our GaAs results in which the effective mass appears to diverge and the Drude oscillator strength vanishes at n_c . Another possibility, however, is that the spectrum has a broad Drude-like absorption that deviates at low frequencies because of localization or Coulomb gap effects near the Fermi energy.² The solid conclusion that we can make is that the $1s-2p$ oscillator strength in this multiple-valley semiconductor collapses much sooner ($n \approx n_c$) compared with the single-valley GaAs system ($n \approx 5n_c$).

We acknowledge useful discussions with F. Koch and J. P. Peng. This work was supported in part by the NSF under Grant No. DMR 8705002.

¹N. F. Mott and E. A. Davis, *Electronic Properties of Non-Crystalline Materials*, 2nd ed. (Clarendon, Oxford, 1979).

²For a review of recent developments, see B. L. Al'tshuler and P. A. Lee, *Phys. Today* **41**, 36 (1988).

³G. A. Thomas, D. H. Rapkine, S. L. Cooper, S.-W. Cheong, A. S. Cooper, L. F. Schneemyer, and J. V. Waszczak, *Phys. Rev. B* **45**, 2474 (1991).

⁴M.-W. Lee, D. Romero, H. D. Drew, M. Shayegan, and B. S. Elman, *Solid State Commun.* **66**, 23 (1988); D. Romero, S. Liu, H. D. Drew, and K. Ploog, *Phys. Rev. B* **42**, 3179 (1990).

⁵S. Liu, H. D. Drew, A. Illiadis, and S. Hadjipanteli, *Phys. Rev. B* **45**, 1155 (1992); S. Liu, D. Romero, and H. D. Drew, in *Proceedings of International Conference on the Physics of Semiconductors*, edited by E. M. Anastassakis and J. D. Joannopoulos (World Scientific, Singapore, 1990).

noopoulos (World Scientific, Singapore, 1990).

⁶See, for example, B. R. Nag, *Electron Transport in Compound Semiconductors* (Springer-Verlag, New York, 1980).

⁷T. F. Rosenbaum, R. F. Miligan, M. A. Paalance, G. A. Thomas, and R. N. Bhatt, *Phys. Rev. B* **27**, 7509 (1983); G. A. Thomas, M. Capizzi, F. Derosa, R. N. Bhatt, and T. M. Rice, *ibid.* **23**, 5472 (1981).

⁸J. F. Koch and J. P. Peng (private communication).

⁹Ye Qin Yi, Dissertation, Technische Universitat, Munchen, Germany (unpublished).

¹⁰H. K. Ng, M. Capizzi, G. A. Thomas, R. N. Bhatt, and A. C. Gossard, *Phys. Rev. B* **33**, 7329 (1986).

¹¹K. Jain, S. Lai, and M. V. Klein, *Phys. Rev. B* **13**, 5448 (1976).